DMD #6742

Determination of the enzyme(s) involved in the metabolism of amiodarone in liver and intestine of rat: The contribution of cytochrome P-450 3A isoforms

Anooshirvan Shayeganpour, Ayman O.S. El-Kadi and Dion R. Brocks

Faculty of Pharmacy and Pharmaceutical Sciences, University of Alberta, Edmonton, Alberta: AS, AOSE and DRB.

Running title: Metabolism of amiodarone in rat

Correspondence to:

Dion R. Brocks, Ph.D.
Associate Professor
Faculty of Pharmacy and Pharmaceutical Sciences
3118 Dentistry/Pharmacy Centre
University of Alberta
Edmonton, AB
Canada
T6G 2N8
e-mail: dbrocks@pharmacy.ualberta.ca
(780) 492-2953   FAX (780) 492-1217

Document Statistics

Number of text pages: 26 (Title page through References)

Number of Tables: 2

Number of Figures: 6

Number of References: 40

Number of words:

  Abstract: 240

  Introduction: 570

  Discussion: 1461

Abbreviations:

AUC, area under the concentration versus time curve; **Cl$_{int}$,** intrinsic clearance; **CL**, total body clearance; **C$_{max}$,** maximum plasma concentration**; CYP**, cytochrome P-450; **HPLC**, high performance liquid chromatography; **k$_i$**, inhibition constant; **k$_m$**, Michelis-Menten affinity constant**; NADPH**, nicotinamide adenine dinucleotide phosphate; **t$_{max}$**, the time at which C$_{max}$ occurs; **Vd**, volume of distribution; **V$_{max}$,** maximum rate of metabolite formation; **Vdss**, volume of distribution at steady state.

Abstract:

In humans, cytochrome p-450 3A (CYP3A4) is a major enzyme involved in the metabolism of amiodarone (AM) to its major metabolite, desethylamiodarone (DEA). In rat, a commonly used animal model, metabolism of AM has not been well studied. To determine if DEA is formed by CYP3A isoenzymes in the rat, microsomal protein was harvested from liver and intestine of male Sprague-Dawley rats. The metabolism of AM in each tissue was assessed utilizing chemical and immunological inhibitors. Ketoconazole, a presumed inhibitor of CYP3A1/2, significantly inhibited formation of DEA by hepatic and intestinal microsomes. However, based on the DEA formation kinetics in both microsomal preparations, it appeared that more than one CYP enzyme was involved in the process. Co-incubation of AM with microsomes and anti-CYP3A2 confirmed the role of CYP3A2 in the metabolism of AM in liver. DEA was also formed by rat recombinant CYP1A1 and CYP3A1, and were inhibited by ketoconazole; hence the participation of these enzymes in the intestinal DEA formation is likely. However, anti-CYP2B1/2 or CYP1A2 antibodies had no effect on DEA formation. In rats given oral or intravenous AM, oral ketoconazole caused significant increases in AUC of oral and i.v. treated rats and over 50% decreases in the CL and Vdss of i.v. treated rats. Although, low to undetectable concentrations of DEA were a limitation for determination of AUC of DEA *in vivo*, it was confirmed that ketoconazole could cause a significant increase in AM concentrations in rat.

Introduction:

Amiodarone (AM) is an iodinated class III antiarrhythmic benzofuran derivative with extensive clinical usage (Trivier et al., 1993; Soyama et al., 2002) in the treatment of life threatening ventricular and supraventricular arrhythmias (Naccarelli et al., 2000). AM undergoes extensive hepatic biotransformation (Trivier et al., 1993; Soyama et al., 2002). Amongst the five pathways involved in the metabolism of AM (N-deethylation, hydroxylation, O-dealkylation, deiodination and glucuronidation), N-dealkylation is most important in humans (Trivier et al., 1993; Soyama et al., 2002). The dealkylated metabolite, desethylamiodarone (DEA) shares some of the pharmacological and toxicological properties of AM. For instance, some of the electrocardiographic changes observed after long term therapy with AM might be related to DEA (Kharidia and Eddington, 1996; Kodama et al., 1999). In addition, both AM and DEA inhibit the intracellular conversion of thyroxine to triiodothyronine. This inhibition may be related to some cardiotoxic effects of AM such as bradycardia and reduced myocardial oxygen consumption, and may explain the hypothyroid-like condition observed after chronic administration of AM (Hudig et al., 1994; Kodama et al., 1999).

AM possesses a very large pharmacokinetic volume of distribution (Vd) and extensive tissue distribution, and in turn, a long terminal half life ($t_{1/2}$) in rat and human plasma (Pollak et al., 2000; Shayeganpour et al., 2005). The drug is also extensively metabolized and has a low hepatic extraction ratio in human (Pollak et al., 2000). In rat, the pharmacokinetics of AM are comparable with humans although clearance was higher in rats (Shayeganpour et al., 2005). Human and rat show different plasma levels of DEA after AM administration, with lower levels being reported in rat compared to human (Wyss et al., 1990; Meng et al., 2001).

In human liver microsomes, an important contribution of CYP3A4 and CYP2C8 isoforms has been demonstrated (Fabre et al., 1993; Trivier et al., 1993). In the human intestine, CYP3A4 is a predominant cytochrome P450 (CYP) enzyme and plays a significant role in the first pass metabolism of 50-70% of marketed drugs (Wacher et al., 1998). In addition, P-glycoprotein (P-gp) is also present at high levels in the villus tip enterocytes of the small intestine (Benet et al., 1999). The presence of CYP3A4 and P-gp in the intestine and their interaction can affect the disposition of drugs that are dual substrates for these proteins (Fabre et al., 1993). It is known that AM is a co-substrate for both P-gp and CYP3A4 (Katoh et al., 2001; Kalitsky-Szirtes et al., 2004). Therefore, oral bioavailability of AM would likely be influenced by presystemic activities of these proteins. Furthermore, inhibition of either of these processes would be predicted to yield higher systemic concentrations of AM, and perhaps lower levels of circulating metabolite(s).

Most current knowledge regarding the metabolism of AM has been obtained from human studies, although some data is available regarding the *in vitro* metabolism of the drug in rabbit and rat (Young and Mehendale, 1986). Nevertheless, little data are available regarding the drug metabolizing enzyme(s) involved in AM biotransformation in the rat, which has been used as an animal model for AM pharmacokinetics (Young and Mehendale, 1986,, Shayeganpour et.al, 2005). The primary objective of this study was to investigate the hepatic and intestinal metabolism of AM to its presumed primary metabolite, DEA, in rat. The influence of ketoconazole (KTZ), a presumed inhibitor of CYP3A1/2 in the rat, was also assessed in vitro and in vivo for its effects on AM metabolism and plasma concentrations.

Materials and Methods

Chemicals

Amiodarone HCl, ethopropazine HCl, ketoconazole, β-nicotinamide adenine dinucleotide phosphate tetrasodium, were purchased from Sigma (St. Louis, Mo, USA). Desethylamiodarone was obtained as a gift from Wyeth Ayerst (Research Monmouth Junction, NJ, USA). Methanol, acetonitrile, hexane (all HPLC grade), triethylamine and sulfuric acid (both analytical grade) were purchased from EM science (Gibstaun, NJ, USA). Potassium dihydrogen orthophosphate, dipotassium hydrogen orthophosphate, potassium chloride, magnesium chloride hexahydrate, sucrose and calcium chloride dihyrate (all analytical grade) were obtained from BDH (Toronto, Ontario, Canada). Halothane BP was purchased from MTC Pharmaceuticals (Cambridge, Ontario, Canada). Heparin sodium injection 1,000 U/ml was obtained from Leo Pharma Inc. (Thornhill, Ontario, Canada). Amiodarone HCl (150 mg/3 ml) as a sterile injectable solution was prepared by Sabex® (Boucherville, Quebec, Canada). Ketoconazole oral tablets (Nizoral®) were purchased from the pharmacy of University of Alberta Hospital (Edmonton, AB, Canada). Anti-rat polyclonal CYP3A2, anti-rat polyclonal CYP2B1/2 raised in rabbit, and anti-rat polyclonal CYP1A2 raised in mouse, were purchased from Daiichi Pure Chemicals Co., Ltd. (Tokyo, Japan). Supersomes expressing either rat CYP1A1 or CYP3A1 with supplementation of cytochrome b_5 and CYP reductase were purchased from BD Gentest (Woburn, MA, USA).

In vitro Studies

Preparation of rat liver and intestinal microsomes

All experimental protocols involving animals were approved by the University of Alberta Health Sciences Animal Policy and Welfare Committee. For *in vitro* studies, eight male Sprague–Dawley rats (Charles River, Quebec, Canada) were sacrificed under halothane anesthesia and their liver and intestinal tissues were excised. Body weight ranged between 250-350 g and all of the rats were housed in temperature controlled rooms with 12 h light per day. For collection of intestinal microsomes, a 25-cm length of duodenum and jejunum

was harvested distal to the beginning of small intestine at the pyloric sphincter. All tissues were washed in ice-cold KCl (1.15 % w/v), cut into pieces and homogenized separately in cold sucrose solution (5 g of tissue in 25 ml of sucrose 0.25 M). Microsomal protein from homogenized tissues was separated by differential ultracentrifugation. The final pellets were collected in cold sucrose and stored at -80°C (Barakat et al., 2001).

Microsomes from four of the rats were prepared separately, and were used to characterize the kinetics of the in vitro formation of DEA from AM, and the effect of KTZ on the DEA formation (chemical inhibition studies, below). The microsomes from the other four rats were pooled and used in the immunoinhibition incubation studies as described below. The Lowry method was used to to measure the total protein concentration in each microsomal preparation (Lowry et al., 1951).

Microsomal incubations

Characterization of DEA formation kinetics

Each 0.5 ml incubate contained 1 mg/ml protein from each of the microsomal preparations from the four individual rats, 0.155-155 µM of AM HCl, 1 mM of NADPH and 5 mM of magnesium chloride hexahydrate dissolved in 0.5M potassium phosphate buffer (pH=7.4). The substrate was added to the liver or intestinal microsomal suspension and the oxidative reactions were started with the addition of NADPH after a 5 min pre-equilibration period. All incubations were performed in quadruplicate in a 37°C water bath shaker for 30 min. Incubation conditions were optimized so that the rate of metabolism was linear with respect to incubation time and microsomal protein concentration.

Chemical inhibition and immunoinhibition studies in rat liver and intestinal microsomes

All of the inhibition studies were accomplished in 16×125 mm flint glass disposable culture tubes. For chemical inhibition studies, KTZ (1.30 to 47.0 µM) was added to microsomal incubations from the individual rats in the presence of different concentrations of AM (16 to 94 µM). The inhibitor (KTZ) was dissolved in methanol. An aliquot of inhibitor was added and tubes were incubated with different concentrations of AM.

In immunoinhibition studies, 20 µl/ml of the CYP3A2, CYP2B1/2 and CYP1A2 antibodies were added separately to the microsomal mixture incubate containing 0.4 mg/ml of pooled microsomal protein and a definite AM concentration (64 and 94 µM for liver and intestine respectively). The percentage of inhibition was determined by comparing the metabolite formation in the presence of antibody to that of matching controls containing preimmune rabbit serum of in place of the antibody.

.

Metabolism by heterogeneously expressed CYP enzymes

To further characterize which P450 in rat mediates the formation of DEA, AM was incubated with a selection of supersomes, which were expressed from rat CYP cDNA using a baculovirus expression system. Incubations were performed with rat recombinant CYP1A1 and CYP3A1. Reactions were carried out at concentrations of 37.6 µM and 18.8 µM for AM and KTZ, respectively. Because this experiment showed linearity in the concentrations between 2-20 pmol/ml of supersomes, a concentration of 10 pmol/ml of each supersome protein was chosen for this experiment.

In vivo studies

Animal and pre-experimental procedures

A total number of 22 male Sprague–Dawley rats (Charles River, Quebec, Canada) were used in *in vivo* drug interaction studies. Body weight ranged between 250-350 g and all of the rats were housed in temperature controlled rooms with 12 h light per day. The animals were fed a standard rodent chow (Lab Diet ® 5001, PMI nutrition LLC, Brentwood, USA). Free access to food and water was permitted prior to experimentation.

Rats were allocated into four groups based on the route of administration and the prior treatment; control i.v. AM (n=6), oral KTZ-i.v. AM (n=6), control oral AM (n=5), and oral KTZ-oral AM (n=5).

The day before the pharmacokinetic experiment, the right jugular veins of all rats were catheterized with Silastic^R (Dow Corning Corporation, Midland,MI, USA) laboratory tubing (0.64×1.19 mm) under halothane anesthesia. Each cannula was flushed with 100 U/ml heparin in 0.9% saline. After cannula implantation, the animals were transferred to regular holding cages and allowed free access to water, but food was withheld overnight. The next morning the rats were transferred to metabolism cages for conduct of the pharmacokinetic experiment.

Drug administration and sample collection

AM injectable solution was used in both intravenous and oral dosing studies. The appropriate doses were prepared by dilution of AM solution in sterile normal saline to a final concentration of 12.5 mg/ml. On the morning of the pharmacokinetic study, i.v. treated rats received 25 mg/kg of AM solution. These doses were injected over 60 s via the jugular vein cannula, immediately followed by injection over 1 min of approximately 1 ml of sterile normal saline solution. Orally-treated rats received 50 mg/kg of AM by oral gavage. Rats treated with KTZ received 17.1

mg/kg of KTZ suspended in 1% of methylcellulose by oral gavage, administered at the time of surgery the day before the experiment, and 0.5 h before and 6 h after AM administration on the day of the pharmacokinetic experiment.

For i.v. studies, blood samples (150-300 µl) were collected approximately at 0.083, 0.33, 0.67, 1, 2, 3, 4, 6, 8, 10, 24, 48 h after the dose administration. In these rats, at the time of first sample withdrawal, the first 0.2-ml volume of blood was discarded. This procedure was shown to have negligible effect on AUC of drug (area under the plasma concentration versus time curve) in rats (Shayeganpour et al., 2005). The sampling times after oral dosage were 0.25, 0.5, 1, 2, 3, 4, 6, 8, 10, 24, 48 h after the dosing. After sample collection, each blood sample was centrifuged at $2500 \times g$ for 3 min and plasma was transferred to a new polypropylene tube and stored at -30° C until analyzed by HPLC.

HPLC Assay

A high performance liquid chromatography (HPLC) method was used for analysis of AM and DEA. The assay had a validated lower limit of quantitation of 35 ng/ml for both AM and DEA based on 100 µL of rat plasma (Shayeganpour and Brocks, 2003; Jun and Brocks, 2001). The method was modified to assay both AM and DEA in microsomal preparations of liver and intestine. Denatured microsomal media were used and spiked for standard curve preparation. Briefly, to the tubes containing 500 µL of microsomal incubation mixture and 1.5 ml of acetonitrile, 30 µL of internal standard (50 µg/ml ethopropazine HCl) was added. The tubes were vortex mixed for 30 seconds and centrifuged for 2 min at 2500 g. The supernatant was transferred to new glass tubes, 7 ml of hexane was added, the tubes vortex mixed for 45 s and centrifuged for 3 min. The organic layer was transferred to new tubes and evaporated to dryness *in vacuo*. The dried residue was reconstituted by adding 125 µl of mobile phase and aliquots of 50 µl were injected into the HPLC. For standard

curve construction, drug free microsomal preparations of liver or intestine were used and spiked with appropriate amounts of AM and DEA. The extraction efficiency of the assay was over 75%.

Data Analysis

The rate of DEA formation in both liver and intestinal microsomes was obtained by plotting the formed DEA at various substrate concentrations. Both single and multiple enzyme models for metabolism of AM to DEA were fitted to the formation rate vs. time data using nonlinear curve fitting routines using an in-house written program based on Microsoft Excel (Microsoft, Redmond WA) and the Solver routine. The Michaelis-Menten model for a single enzyme was used (Venkatakrishnan et al., 2003) as follows:

$$Rate\ of\ DEA\ formation = \frac{V_{max} \times [AM]^n}{k_m{}^n + [AM]^n} \qquad \text{Eq. 1}$$

Where V_{max} is the maximal rate of formation (capacity), k_m is the affinity constant, [AM] is the concentration of AM and n is the shape factor required to fit sigmoidal shapes. When n=1 the model reduced to the simple Michaelis Menten equation.

One of the two enzyme-models that was used consisted of a single saturable and a second linear component (Venkatakrishnan et al., 2003), as follows:

$$Rate\ of\ DEA\ formation = \frac{V_{max1} \times [AM]}{k_{m1} + [AM]} + E_2 \times [AM] \qquad \text{Eq. 2}$$

Where k_{m1} and V_{max1} were the kinetic constants for a high affinity enzyme, and E_2 represented the V_{max}/k_m ratio for the low affinity enzyme. The optimal choice of enzyme model was judged by the residual sum of squares and the Akaike Information Criterion.

The simple competitive inhibition model was considered for the effects of KTZ as defined in the equation below, with k_i as the dissociation constant of the inhibitor-enzyme complex) and [I] the inhibitor concentration.

$$k_{m(1)} = k_{m(1)} \times (1 + \frac{[I]}{k_i})$$
Eq. 3

The k_i value in liver was determined by Dixon plot analysis (Dixon, 1953; Cortes et al., 2001).

For the pharmacokinetic studies, noncompartmental methods were used to calculate the parameters of maximal plasma concentration (C_{max}) and time thereof (t_{max}), clearance (CL), volume of distribution at steady-state (Vdss), terminal elimination rate constant and half-life ($t_{\frac{1}{2}}$), as previously described (Shayeganpour et al., 2005). The log-linear trapezoidal rule was used to calculate the area under the plasma concentration vs. time curve.

Statistical Analysis

Compiled data are expressed as mean±SD unless otherwise indicated. One way ANOVA, Duncan's Multiple Range *post hoc* test and Student paired or unpaired t-tests were used as appropriate to assess the significance of differences between groups. Microsoft Excel or SPSS version 12 (SPSS Inc., Chicago, IL) were used in statistical analysis of data. The level of significance was set at $p < 0.05$.

Results

Metabolism of AM by liver and intestinal microsomes

In both liver and intestine, as AM concentrations increased there was an increase in the formation rate of DEA. It was found that in liver microsomes, the kinetic profile of DEA formation vs. concentration conformed well to the Michaelis-Menten model with one enzyme (Figure 1A). However there did appear to be some deviation from the model with the highest mean concentration. The estimated k_m, V_{max} and intrinsic clearance (CL_{int}) were determined in liver (Table 1). The variability assessed by coefficient of variation was substantially higher for k_m (74%) than V_{max} (21%).

In contrast to liver microsomes, over the range of concentrations studied, a linear model best fit the DEA formation vs. AM concentration relationship ($r^2 > 0.99$) in intestinal microsomes (Figure 1B). As a result, determination of k_m, V_{max} and CL_{int} was not possible in these microsomes.

Identification of the CYP isoenzymes responsible for the metabolism of AM to DEA

To identify the CYP isoenzymes involved in the metabolism of AM to DEA, chemical inhibition, anti-CYP antibodies and recombinant rat CYP enzymes were employed. To further establish the role of CYP1A1 and CYP3A1 in the metabolism of AM to DEA, AM was incubated with recombinant rat CYP1A1 and CYP3A1 enzymes. As the concentration of KTZ was increased in the chemical inhibition study (Figure 2A), a progressive decrease was noted in the formation rate of DEA in rat liver microsomes. In comparison to control incubations, all of the incubations in which KTZ was added yielded significantly lower DEA formation rates, for each of the three AM concentrations studied (Figure 2). In general, as KTZ concentrations were increased, there were significant decreases in formation rates of DEA.

In intestinal microsomes (Figure 2B), increasing concentrations of KTZ did not seem to have the same effects on DEA formation. At the highest concentration of AM exposed to intestinal microsomes, no significant difference was observed in the formation of metabolite with increasing concentrations of inhibitor (Figure 2B). Similar to liver, at lower concentrations of AM (23.5 and 47 µM), the formation of DEA in intestine was significantly lower than control incubations when KTZ was present. There was, however, a difference in the pattern of effect of KTZ in intestine as compared to liver, because in intestine KTZ did not result in a markedly progressive decrease in DEA formation at KTZ concentrations above 1.88 µM (Figure 2B).

The inhibition constant, ki, was determined by the use of Dixon plot analysis in the liver microsomes (Figure 3). The one enzyme model did not fit well to the inhibition data, so a two enzyme model was used, with involvement of a high affinity and a low affinity enzyme (Eq. 2). This model provided an optimal fit to the data, and was used to estimate the ki for the inhibition of DEA by KTZ (Figure 3). Based on this two enzyme kinetic model, ki was determined to be 2.74±3.50 µM of KTZ (range, 0.391 to 7.94 µM). This analysis was not possible in intestinal microsomes due to poor quality of the fit of the model to the data.

Anti-CYP1A2, CYP3A2, CYP2B1/2 antibodies were employed to better identify the CYP enzymes involved in the metabolism of AM in liver and intestine microsomes. No significant differences were observed in the formation of DEA with CYP1A2 and CYP2B1/2 antibodies in both liver and intestine microsomes (Figure 4). However, the formation of DEA was significantly decreased in using anti-CYP3A2 in liver, but not intestinal microsomes.

When AM was incubated in the presence of rat CYP1A1 and CYP3A1 supersomes, DEA was observed to be formed in both cases (Figure 5). In addition, when KTZ (18.8 μM) was added, significant decreases were observed in the formation rate of DEA.

Pharmacokinetics of AM in rats

KTZ pretreatment gave rise to a significant increase in plasma concentrations of i.v. administered AM in comparison with control rats. In rats given AM orally, significant increases were also detected in systemic disposition of AM upon administration of KTZ (Figure 6). After i.v. doses of AM, the mean plasma AUC_{0-48} and $AUC_{0-\infty}$ were increased 1.67 and 1.60–fold respectively in KTZ treated rats compared to the control animals (Table 2). The CL and Vdss of AM in KTZ treated rats were significantly lower than that of control rats. No significant difference was observed in the $t_{1/2}$ of i.v. AM in the presence and absence of KTZ (Table 2).

Compared to control animals, KTZ caused 3.07- and 2.06-fold increases in AUC_{0-48} and $AUC_{0-\infty}$ respectively, in the rats given AM orally. Administration of KTZ led to a substantial increase (137%) in C_{max} of AM after its oral administration (Table 2, Figure 6). No significant differences were observed in $t_{1/2}$ and t_{max} of AM with or without treatment of KTZ (Table 2). Using $AUC_{0-\infty}$, the oral bioavailabilities of AM (F) were estimated to be 37% and 47% in control and KTZ treated rats respectively. Similar estimates of F were obtained if partial AUC was used from 0-48 h (28% and 52% in control and KTZ-treated rats, respectively).

The mean C_{max} of DEA was considerably lower than that of AM in each of the groups (Table 2). There were no differences between KTZ-treated and control animals given either i.v. or oral AM (Table 2). Although the amounts of DEA detected in some plasma samples were greater than the lower limit of quantification of the assay (35 ng/ml), many of the samples were not

quantifiable for DEA. Hence, a complete plasma concentration vs. time profile of DEA concentration was not obtained in most of the rats, and the AUC could not be reported.

Discussion

The role of CYP in the biotransformation of AM to DEA and its first pass elimination in different tissues such as liver, kidney, intestine and lung has attracted attention (Rafeiro et al., 1990; Kalitsky-Szirtes et al., 2004). In the present study the role of hepatic and intestinal microsomes in biotransformation of AM to DEA was attempted. The study findings demonstrated a considerable difference between rat liver and intestinal microsomes in their ability to metabolize AM to DEA. Over the range of concentrations studied, liver microsomal protein showed a consistently higher rate of metabolism than intestinal microsomes (Figure 1). Kinetic constants could be reasonably derived for the metabolism of AM in liver using the single enzyme Michaelis Menten model, but this was not the case for intestinal microsomes. However it was of note that in liver microsomes, there appeared to be some deviation from the model with the highest mean concentration, and in three of the four livers, Eadie-Hofstee plots (Venkatakrishnan et al., 2003) suggested the possibility of more than one enzyme being involved in liver formation of DEA. Given the linearity over the range of concentrations studied in intestinal microsomes (Figure 1), it appears that the enzymes involved in metabolism of AM to DEA in intestine have a markedly lower affinity for AM than those in liver. This implied that there were tissue- specific enzymes involved in the formation of DEA. To our knowledge, there are no available reports describing the metabolism of human intestinal microsomes for comparison with our rat data.

In microsomes isolated from human livers, it has been reported that the mean V_{max}, k_m and Cl_{int} were 68.7 pmol/min/mg protein, 38.9 µM, and 1.76 µL/min/mg protein, respectively (Trivier et al., 1993). In comparison, in our study, the V_{max}, k_m and CL_{int} in rat livers were

observed to be 5.4-fold, 1.1-fold and 5.4-fold higher than in those values reported for human liver (Table 1). This is consistent with the higher total body CL noted in rats (23 ml/min/kg) (Shayeganpour et al., 2005) vs. humans (range of means: 1.9 to 8.2 ml/min/kg) (Anastasiou-Nana et al., 1982; Riva et al., 1982; Vadiei et al., 1997).

Based on the differential findings in the kinetic profiles between liver and intestinal formation of DEA from AM, it appeared there was more than one enzyme involved in the biotransformation, which warranted further study. Guengerich and Schimada proposed five different *in vitro* approaches for elucidation of catalytic activities of CYP4540 in human liver (Guengerich and Shimada, 1991). In our study we selected three of these approaches to better identify the responsible enzymes. These included inhibition by a presumed chemical inhibitor of CYP3A in rat (KTZ), immunoinhibition and supersomes.

In liver as the concentrations of KTZ were increased, there was a progressive decrease observed in the formation rate of DEA irrespective of the concentration of AM initially present (Figure 2A). In intestinal microsomes containing either 23.5 or 47 µM of AM, this pattern differed, in that there was a decline in rate with a low concentration of KTZ, but with additional amounts of KTZ there was no perceptible enhancement in the inhibition of DEA formation (Figure 2B). Clearly there was a difference in the involved CYP enzymes in this biotransformation between these two tissues, and suggests the involvement of different CYP in the formation of DEA from the parent drug, AM.

Although KTZ has been identified to be a selective inhibitor of CYP3A4 in human microsomes (Eagling et al., 1998; Turan et al., 2001), it has been reported that in rat KTZ is not as selective an inhibitor of CYP3A (Eagling et al., 1998). Employment of Dixon plots for determination of ki suggested that there are two CYP enzymes involved in the metabolism

of AM in rat liver microsomes (Figure 3). The inhibition data fit well to a two enzyme model, where one enzyme was high capacity and high affinity, and the second was low capacity and low affinity for AM. Incubation of microsomes with anti-CYP antibodies indicated that in liver, but not intestine, CYP3A2 was involved in the formation of DEA from parent drug. There were no decreases noted in the formation of DEA in the presence of antibodies to CYP1A2 and 2B1/2, respectively, suggesting that these enzymes are not involved in this biotransformation (Figure 4).

CYP1A1 is a metabolic enzyme responsible for chemical activation of xenobiotics to carcinogenic derivatives in some extrahepatic tissues such as lung (Zhao et al., 2004; Gharavi and El-Kadi, 2005). Use of supersomes established a role for CYP1A1 and CYP3A1 in the formation of DEA (Figure 5). In addition, both of these enzymes were significantly inhibited by the addition of KTZ. The inhibition by KTZ of CYP1A1 was more marked (96%) than that of CYP3A1 (78%). Due to high expression of CYP1A1 and CYP3A1 in rat intestine (Zhang et al., 1996; Turan et al., 2001; Kaminsky and Zhang, 2003), we can conclude that the aforementioned enzymes are involved in the metabolic biotransformation of AM to DEA in intestine. It is of note that in addition to intestine, CYP1A1 is also an important enzyme found in lung (Seubert et al., 2002; Zhao et al., 2004). Furthermore, high expression of CYP1A1, CYP1A2, CYP2B1, CYP3A1 and CYP3A2 has been shown to occur constitutively within small hepatocytes of adult rats . The ability of KTZ to inhibit intestinal CYP1A1 activity in humans has previously been demonstrated (Paine et al., 1999).

Our previously calculated high extraction ratio of AM reported in rat (Shayeganpour et al., 2005) incorporates both hepatic and extrahepatic elimination in other tissues such as intestine, lung or kidney. Based on previous reports (Wyss et al., 1990; Shayeganpour et

al., 2005) circulating DEA levels in the rat are much lower than those observed in human (Meng et al., 2001). This could be due to this pathway being of minor importance in the elimination of AM in the rat. Alternatively, the low concentrations of DEA observed in the rat may be due to a faster CL and perhaps larger Vd of DEA in comparison to AM. To our knowledge there are no reports of DEA CL or Vdss in rats after i.v. dosing. To assess the relevance of the *in vitro* findings, we undertook an *in vivo* experiment to determine the effect of KTZ inhibition on AM pharmacokinetics.

As previously observed (Shayeganpour et al., 2005), the concentrations of DEA were near the lower limit of quantitation of the assay in all groups of rats after i.v. and oral administration of AM. Nevertheless, administration of oral KTZ caused significant increases (1.60-fold) in the $AUC_{0-\infty}$ and a decrease (1.56-fold) in CL of AM after i.v. administration of AM (Table 2, Figure 6A). Furthermore, there was an unexpected decrease (2-fold) in the Vdss of KTZ-treated vs. control rats (Table 2). A similar finding has been observed in other studies involving nifedipine, docitaxel and almotriptan co-administered with KTZ. The concomitant administration of oral KTZ and i.v. administration of 0.5 mg/kg nifedipine to dogs showed 1.83-fold increase in AUC, and 1.73 and 1.2- fold decreases in the CL and Vdss respectively (Kuroha et al., 2002) Similarly, co-administration of 12.5 mg of almotriptan, a selective 5-HT$_{1B/1D}$ agonist, and 400 mg KTZ to healthy volunteers generated a 44% decrease in the Vz/F of almotriptan (Fleishaker et al., 2003). In subjects given KTZ (200 mg/day for 3 consecutive days orally) with docitaxel (10 mg/m^2), an 18.7% decrease in docitaxel Vdss was reported (Engels et al., 2004). The underlying reasons for these observations have not been addressed. The possibility of a displacement interaction at the level of tissue binding, or an increase in the capacity and/or affinity of binding to plasma proteins, could explain the results.

After oral administration of AM, the effects of KTZ on exposure to AM were greater than those observed after its i.v. administration (Table 2, Figure 6B). Given the demonstrated ability of AM to be metabolized by rat intestine (Figure 1B, Table 1), this is perhaps not surprising. KTZ is recognized as a dual P-gp/CYP3A1 inhibitor (Ward et al., 2004), and AM is also identified as a substrate of P-gp (Kalitsky-Szirtes et al., 2004). In addition to inhibition of intestinal CYP3A1, the additional contribution of inhibition of intestinal CYP1A1 and reduced P-gp mediated efflux are likely contributors to the increased oral bioavailability after co-administration of AM with KTZ.

In conclusion, the current results demonstrate that both liver and intestine play an important role in the first pass metabolism of AM. Liver microsomal protein was more efficient at forming DEA than intestinal microsomes. Furthermore, we confirmed a role of CYP3A1, CYP3A2 and CYP1A1 in metabolism of AM to DEA in both liver and intestine of rat species. In addition, our pharmacokinetic studies demonstrated that oral administration of KTZ caused increased concentrations of AM presumably by inhibition of CYP1A1 and 3A1.

References

Anastasiou-Nana M, Levis GM and Moulopoulos S (1982) Pharmacokinetics of amiodarone after intravenous and oral administration. *Int J Clin Pharmacol Ther Toxicol* **20:**524-529.

Barakat MM, El-Kadi AO and du Souich P (2001) L-NAME prevents in vivo the inactivation but not the down-regulation of hepatic cytochrome P450 caused by an acute inflammatory reaction. *Life Sci* **69:**1559-1571.

Benet LZ, Izumi T, Zhang Y, Silverman JA and Wacher VJ (1999) Intestinal MDR transport proteins and P-450 enzymes as barriers to oral drug delivery. *J Control Release* **62:**25-31.

Cortes A, Cascante M, Cardenas ML and Cornish-Bowden A (2001) Relationships between inhibition constants, inhibitor concentrations for 50% inhibition and types of inhibition: new ways of analysing data. *Biochem J* **357:**263-268.

Dixon M (1953) The determination of enzyme inhibitor constants. *Biochem J* **55:**170-171.

Eagling VA, Tjia JF and Back DJ (1998) Differential selectivity of cytochrome P450 inhibitors against probe substrates in human and rat liver microsomes. *Br J Clin Pharmacol* **45:**107-114.

Engels FK, Ten Tije AJ, Baker SD, Lee CK, Loos WJ, Vulto AG, Verweij J and Sparreboom A (2004) Effect of cytochrome P450 3A4 inhibition on the pharmacokinetics of docetaxel. *Clin Pharmacol Ther* **75:**448-454.

Fabre G, Julian B, Saint-Aubert B, Joyeux H and Berger Y (1993) Evidence for CYP3A-mediated N-deethylation of amiodarone in human liver microsomal fractions. *Drug Metab Dispos* **21:**978-985.

Fleishaker JC, Herman BD, Carel BJ and Azie NE (2003) Interaction between ketoconazole and almotriptan in healthy volunteers. *J Clin Pharmacol* **43:**423-427.

Gharavi N and El-Kadi AO (2005) tert-Butylhydroquinone is a novel aryl hydrocarbon receptor ligand. *Drug Metab Dispos* **33:**365-372.

Guengerich FP and Shimada T (1991) Oxidation of toxic and carcinogenic chemicals by human cytochrome P-450 enzymes. *Chem Res Toxicol* **4:**391-407.

Hudig F, Bakker O and Wiersinga WM (1994) Amiodarone-induced hypercholesterolemia is associated with a decrease in liver LDL receptor mRNA. *FEBS Lett* **341:**86-90.

Jun AS and Brocks DR (2001) High-performance liquid chromatography assay of amiodarone in rat plasma. *J Pharm Pharm Sci* **4:**263-268.

Kalitsky-Szirtes J, Shayeganpour A, Brocks DR and Piquette-Miller M (2004) Suppression of drug-metabolizing enzymes and efflux transporters in the intestine of endotoxin-treated rats. *Drug Metab Dispos* **32:**20-27.

Kaminsky LS and Zhang QY (2003) The small intestine as a xenobiotic-metabolizing organ. *Drug Metab Dispos* **31:**1520-1525.

Katoh M, Nakajima M, Yamazaki H and Yokoi T (2001) Inhibitory effects of CYP3A4 substrates and their metabolites on P-glycoprotein-mediated transport. *Eur J Pharm Sci* **12:**505-513.

Kharidia J and Eddington ND (1996) Effects of desethylamiodarone on the electrocardiogram in conscious freely moving animals: pharmacokinetic and pharmacodynamic modeling using computer-assisted radio telemetry. *Biopharm Drug Dispos* **17:**93-106.

Kodama I, Kamiya K and Toyama J (1999) Amiodarone: ionic and cellular mechanisms of action of the most promising class III agent. *Am J Cardiol* **84:**20R-28R.

Kuroha M, Kayaba H, Kishimoto S, Khalil WF, Shimoda M and Kokue E (2002) Effect of oral ketoconazole on first-pass effect of nifedipine after oral administration in dogs. *J Pharm Sci* **91:**868-873.

Lowry OH, Rosebrough NJ, Farr AL and Randall RJ (1951) Protein measurement with the Folin phenol reagent. *J Biol Chem* **193:**265-275.

Meng X, Mojaverian P, Doedee M, Lin E, Weinryb I, Chiang ST and Kowey PR (2001) Bioavailability of amiodarone tablets administered with and without food in healthy subjects. *Am J Cardiol* **87:**432-435.

Naccarelli GV, Wolbrette DL, Dell'Orfano JT, Patel HM and Luck JC (2000) Amiodarone: what have we learned from clinical trials? *Clin Cardiol* **23:**73-82.

Paine MF, Schmiedlin-Ren P and Watkins PB (1999) Cytochrome P-450 1A1 expression in human small bowel: interindividual variation and inhibition by ketoconazole. *Drug Metab Dispos* **27:**360-364.

Pollak PT, Bouillon T and Shafer SL (2000) Population pharmacokinetics of long-term oral amiodarone therapy. *Clin Pharmacol Ther* **67:**642-652.

Rafeiro E, Leeder RG, Daniels JM, Brien JF and Massey TE (1990) In vitro hepatic, renal, and pulmonary N-dealkylation of amiodarone. *Biochem Pharmacol* **39:**1627-1629.

Riva E, Gerna M, Latini R, Giani P, Volpi A and Maggioni A (1982) Pharmacokinetics of amiodarone in man. *J Cardiovasc Pharmacol* **4:**264-269.

Seubert JM, Sinal CJ and Bend JR (2002) Acute sodium arsenite administration induces pulmonary CYP1A1 mRNA, protein and activity in the rat. *J Biochem Mol Toxicol* **16:**84-95.

Shayeganpour A and Brocks DR (2003) Joint assay of desethylamiodarone and amiodarone by high performance liquid chromatography. *Journal of Pharmacy and Pharmaceutical Sciences* **6:**160.

Shayeganpour A, Jun AS and Brocks DR (2005) Pharmacokinetics of Amiodarone in hyperlipidemic and simulated high fat-meal rat models. *Biopharm Drug Dispos* **26:**249-257.

Soyama A, Hanioka N, Saito Y, Murayama N, Ando M, Ozawa S and Sawada J (2002) Amiodarone N-deethylation by CYP2C8 and its variants, CYP2C8*3 and CYP2C8 P404A. *Pharmacol Toxicol* **91:**174-178.

Trivier JM, Libersa C, Belloc C and Lhermitte M (1993) Amiodarone N-deethylation in human liver microsomes: involvement of cytochrome P450 3A enzymes (first report). *Life Sci* **52:**PL91-96.

Turan VK, Mishin VM and Thomas PE (2001) Clotrimazole is a selective and potent inhibitor of rat cytochrome P450 3A subfamily-related testosterone metabolism. *Drug Metab Dispos* **29:**837-842.

Vadiei K, Troy S, Korth-Bradley J, Chiang ST and Zimmerman JJ (1997) Population pharmacokinetics of intravenous amiodarone and comparison with two-stage pharmacokinetic analysis. *J Clin Pharmacol* **37:**610-617.

Venkatakrishnan K, von Moltke LL, Obach RS and Greenblatt DJ (2003) Drug metabolism and drug interactions: application and clinical value of in vitro models. *Curr Drug Metab* **4:**423-459.

Wacher VJ, Silverman JA, Zhang Y and Benet LZ (1998) Role of P-glycoprotein and cytochrome P450 3A in limiting oral absorption of peptides and peptidomimetics. *J Pharm Sci* **87:**1322-1330.

Ward KW, Stelman GJ, Morgan JA, Zeigler KS, Azzarano LM, Kehler JR, McSurdy-Freed JE, Proksch JW and Smith BR (2004) Development of an in vivo preclinical screen model to estimate absorption and first-pass hepatic extraction of xenobiotics. II. Use of ketoconazole to identify P-glycoprotein/CYP3A-limited bioavailability in the monkey. *Drug Metab Dispos* **32:**172-177.

Wyss PA, Moor MJ and Bickel MH (1990) Single-dose kinetics of tissue distribution, excretion and metabolism of amiodarone in rats. *J Pharmacol Exp Ther* **254:**502-507.

Young RA and Mehendale HM (1986) In vitro metabolism of amiodarone by rabbit and rat liver and small intestine. *Drug Metab Dispos* **14:**423-429.

Zhang QY, Wikoff J, Dunbar D and Kaminsky L (1996) Characterization of rat small intestinal cytochrome P450 composition and inducibility. *Drug Metab Dispos* **24:**322-328.

Zhao HW, Barger MW, Ma JK, Castranova V and Ma JY (2004) Effects of exposure to diesel exhaust particles (DEP) on pulmonary metabolic activation of mutagenic agents. *Mutat Res* **564:**103-113.

Footnotes

Legends for Figures

Figure 1-Rate (mean ± SD) of DEA formation in liver (A) and intestinal (B) microsomes of four individual Sprague-Dawley rats after 30 min incubation with increasing concentration of AM (x-axis).

Figure 2- Effect of increasing concentrations of ketoconazole on DEA formation (y-axis) in microsomes from four individual rats, in the presence of three concentrations of AM. A. Liver microsomes, B. Intestinal microsomes. Breaks between horizontal lines above data bars denote significant differences from other data at the same concentration of AM (Duncan's multiple range *post-hoc* test).

Figure 3- Determination of ki (2.74±3.50 μM) in liver microsomes by Dixon plot. Inhibition data (see Figure 2) was fitted to a two enzyme model (combined Eq. 2 and 3), with results of model fits being represented by the solid lines.

Figure 4. Immunoinhibition studies in liver and intestinal (gut) microsomal protein (0.4 mg/ml) pooled from four rats, coincubated with amiodarone (64 and 94 μM for liver and intestine respectively) and antibodies to either A.) CYP1A2; B.) CYP2B1/2 or C.) CYP3A2. Matching control incubations without antibody are shown. *Denotes significant difference from corresponding control incubation.

Figure 5- Formation of DEA from 37.6 μM AM in the presence of CYP1A1 or CYP3A1 supersomes, in the absence (control) and presence of 18.8 μM ketoconazole (KTZ). *Denotes significant difference from corresponding control incubation.

Figure 6- Mean ± SD plasma concentration versus time profile of amiodarone with and without treatment with ketoconazole after A.) single 25 mg/kg intravenous or B.) 50 mg/kg oral doses of amiodarone HCl.

Table 1- Enzyme kinetic parameters for desethylamiodarone formation by rat liver microsomes from four individual rats, based on results of fit of Eq. 2 to the data.

| Kinetic parameter	Mean±SD (range)
Km (μM)	43.5±32.1 (24.3-70.2)
V_{max} (pmol/min/mg protein)	370±78.4 (250-463)
CL_{int} (μL/min/mg protein)	9.51±3.42 (4.74-12.8)

Table 2- Pharmacokinetic parameters (mean±SD, range in parenthesis) of amiodarone and desethylamiodarone after i.v. and oral administration in rats in the absence (controls) and presence of oral ketoconazole (17.1 mg/kg $\times$ 3 doses over 1 day).

Intravenous (25 mg/kg AM HCl)		Oral (50 mg/kg AM HCl)	
Control (n=6)	*KTZ (n=6)*	*Control(n=5)*	*KTZ(n=5)*
AUC_{0-48h}, mg$\times$h/l			
15.4±2.90	25.6±6.02[a]	8.73±1.98	26.8±9.03[a]
(12.6-19.5)	(20.6-34.1)	(7.06-12.0)	(17.7-36.8)
$AUC_{0-\infty}$ (mg$\times$h/L)			
18.5±3.27	29.6±7.49[a]	13.6±6.97	28.0±9.46[a]
(13.4-23.0)	(22.2-41.5)	(8.11-24.1)	(18.3-39.3)
CL (ml/h/kg)			
1390±269	889±209[a]	-	-
(1086-1860)	(602-1126)		
Vdss (L/kg)			
40.9±19.7	20.2±9.47[a]	-	-
(22.1-51.5)	(9.01-37.0)		
$t_{1/2}$ (h)			
39.4±24.2	30.1±21.5	32.2 ± 21.9	9.93 ±1.31
(17.2-78.8)	(10.1-59.5)	(16.9-69.8)	(8.21-11.3)
C_{max} (ng/ml)			
-	-	723±355	1716±495[a]
		(317-1123)	(1329-2296)
Median t_{max}(h)			
-	-	5.93	8.00
		(2.18-10.1)	(2.08-10.3)
Desethylamiodarone pharmacokinetics parameters			
C_{max} (ng/ml)			
66.2±50.0	86.1±55.1	49.1±29.5	138±93.3
Median t_{max} (h)			
0.369	24.4	5.93	10.0
(0.083-3.7)	(0.116-49.3)	(3.21-10.2)	(6.06-10.5)

[a] Denotes significantly difference from similarly dosed control rats

Figure 1
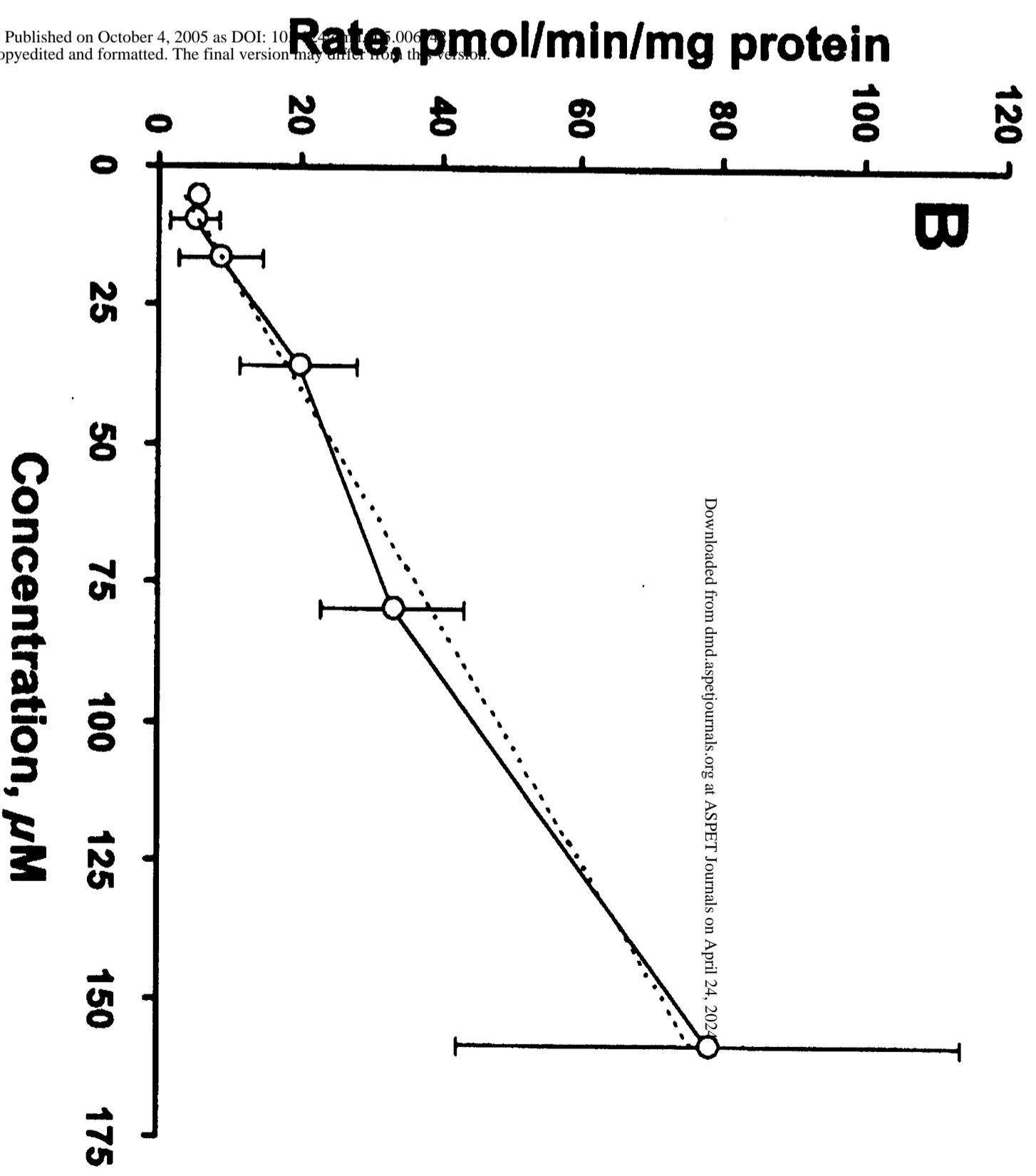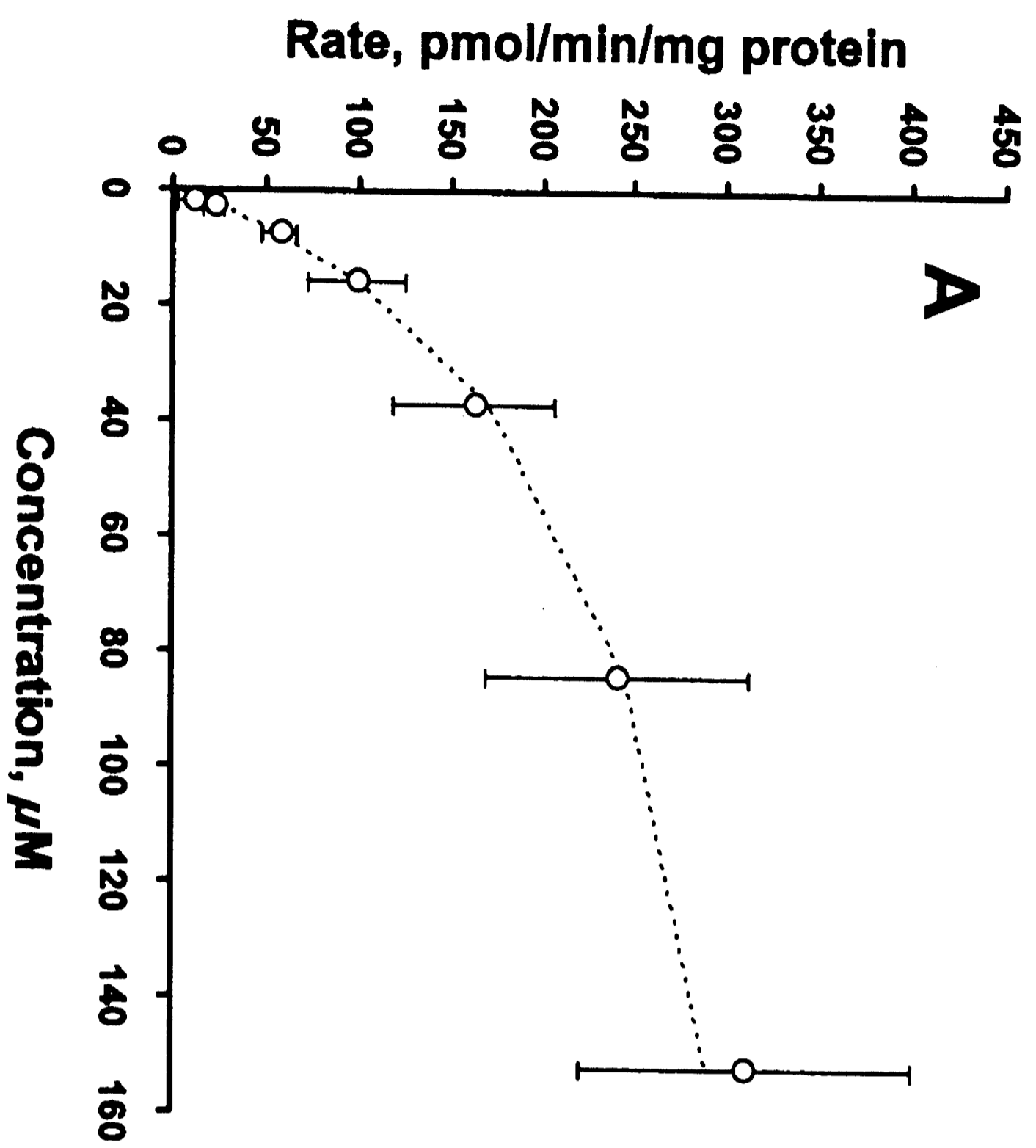
Rate, pmol/min/mg protein

Concentration, μM

A

Rate, pmol/min/mg protein

Concentration, μM

B
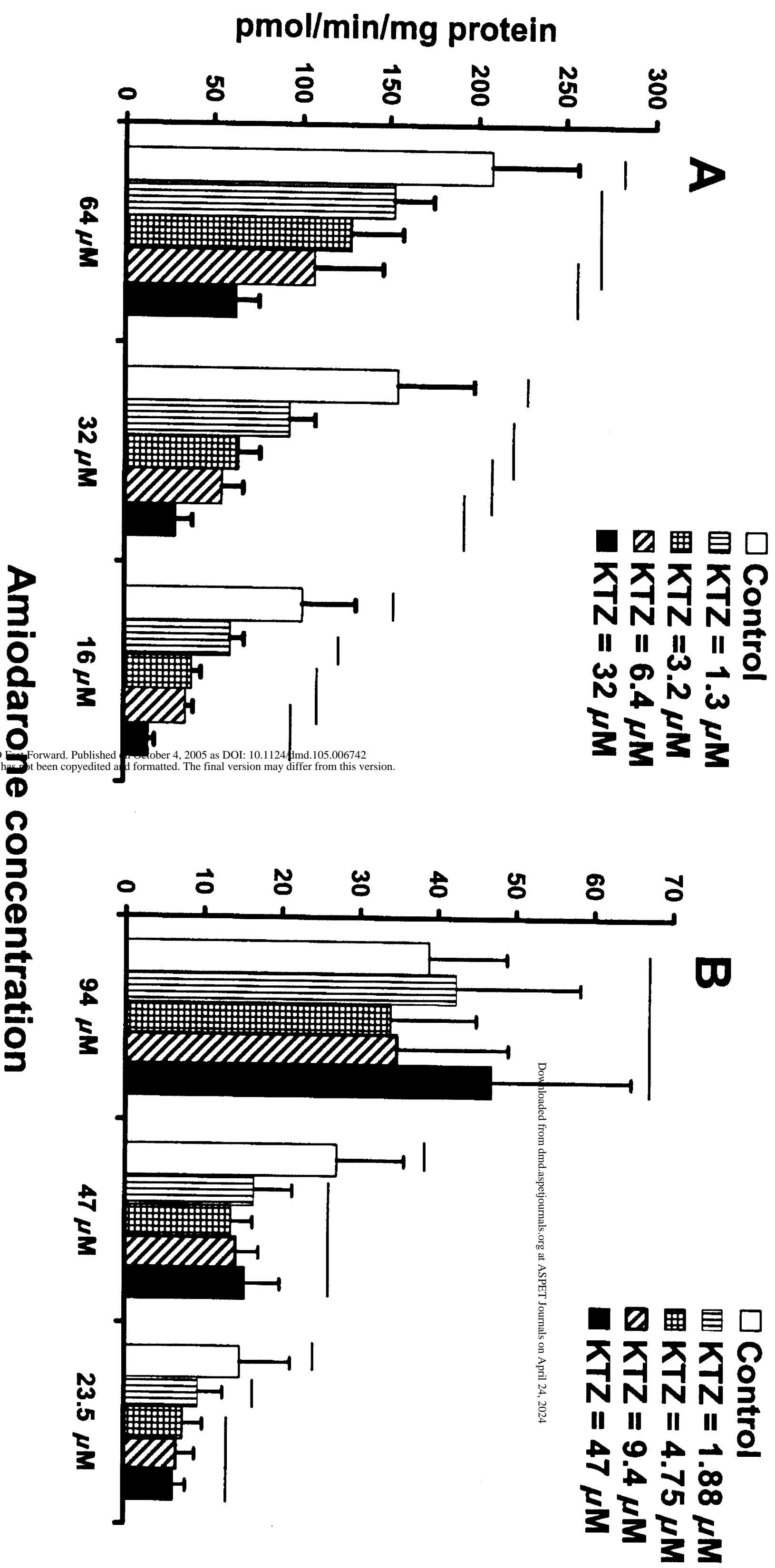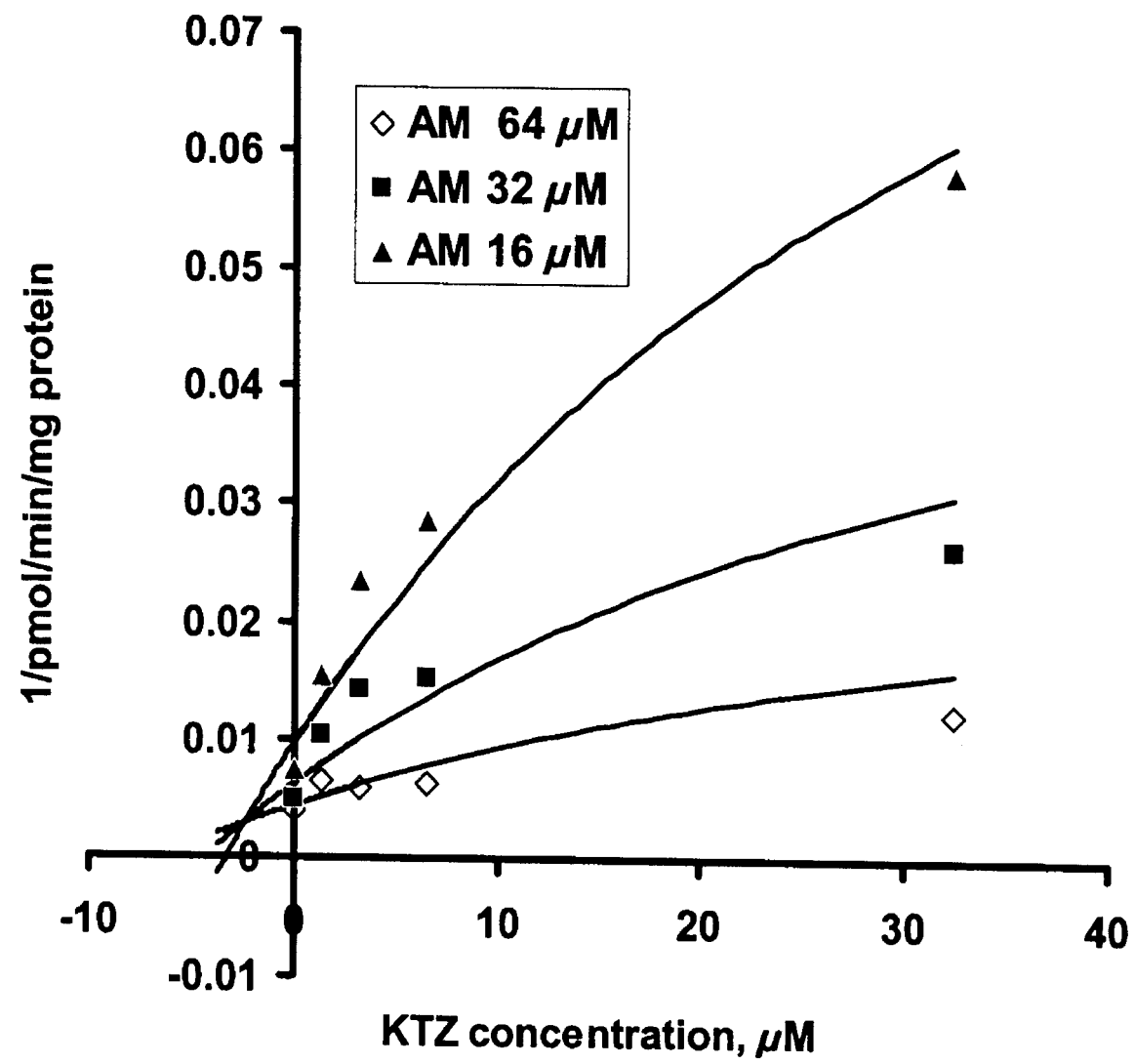
Figure 2

Figure 3

Figure 4

Figure 5

Figure 6